

Nanolayered TiN/NbN Multilayers as New Superhard Materials

Author's Corrections:

Received on:	
Mailed back on:	
Initial	

Harish C. Barshilia and K.S. Rajam

Surface Engineering Division, National Aerospace Laboratories

Post Bag No. 1779, Bangalore - 560 017

India

E-mail: harish@css.cmmacs.ernet.in and rajam@css.cmmacs.ernet.in

Abstract

Nanolayered multilayer coatings of TiN/NbN on silicon and tool steel substrates were deposited using a reactive DC magnetron sputtering process. Judicious control of process parameters enabled the deposition of stoichiometric TiN/NbN coatings. The bilayer thickness, also known as modulation wavelength (L), critically affected the properties of the coatings. Coatings deposited at $150 \text{ \AA} \leq L \leq 30 \text{ \AA}$ exhibited superlattice structure as evidenced by XRD. Nanoindentation data indicated that polycrystalline TiN/NbN multilayers exhibited hardness as high as 4000 kg/mm^2 , which was ~ 2 times the rule-of-mixtures value. Annealing of the coatings in vacuum indicated that coatings retained superlattice structure even up to 850°C . Furthermore, the multilayer coatings showed a tremendous improvement in the corrosion resistance in 0.5 M HCl solution as compared to the single layer TiN and NbN coatings.

1.0 Introduction

Multilayer coatings have attained a considerable interest because of their exotic mechanical properties. Nanostructured multilayer coatings of ceramic materials (especially those of transition metal nitrides) are an emerging class of superhard materials.¹⁻⁴ In these coatings, alternate layers of two materials (e.g., TiN and NbN) are deposited onto a substrate; the thicknesses of individual layers being on the atomic scale. The thickness of each successive pair of layers is commonly known as modulation wavelength (Λ), which critically affects the properties of the multilayers. Nanostructured multilayer coatings are also commonly known as superlattices. Because of very small layer thicknesses and presence of a large number of interfaces these materials exhibit exotic mechanical properties. For example, hardness as high as $4000\text{--}5000 \text{ kg/mm}^2$ has been reported for TiN/NbN multilayer coatings, which is very high as compared to rule-of-mixtures value.^{3,5} Layering of the two materials not only improves mechanical properties but also the chemical and thermal stability of the coatings. Furthermore, these coatings can be deposited at low

temperatures with excellent adhesion to most of the engineering substrates. Superlattice coatings are not only important for technological applications but also very important scientific issues related to the enhancement in their physical properties need to be addressed.

TiN/NbN multilayer system is technologically important since it is expected to have lower residual stresses apart from the superior mechanical properties.⁵ TiN/NbN coatings are also thermally stable at higher temperatures.³ Deposition of multilayer coatings of TiN/NbN is difficult because the heat of formation of NbN (56.2 kcal/mol) is considerably less than that of TiN (80.8 kcal/mol). Different partial pressures of nitrogen are, thus, required in the same deposition chamber to deposit stoichiometric TiN and NbN coatings. Another problem is that niobium nitride exists in cubic ($\alpha\text{-NbN}$) and hexagonal ($\beta\text{-Nb}_2\text{N}$) phases.⁶ In a reactive sputtering process judicious control of process parameters, such as - nitrogen partial pressure, target power, energy and flux of ions, is essential to achieve high performance coatings. In this article, we briefly describe the growth of TiN/NbN superlattices. X-ray diffraction (XRD) has been used to study

the structural properties of the coatings. In brief, the mechanical properties of the coatings, as measured by a nanoindentation technique, have been presented. Thermal and chemical stability of the coatings are also discussed.

2.0 Experimental Procedure

Alternate layers of TiN and NbN of varying thicknesses (20–300 Å) were deposited on Si (111) single crystal and tool steel composition of the tool steel used substrates using a reactive DC planar magnetron sputtering system that has been described in detail elsewhere.^{2–4,7} In order to get varying thicknesses of TiN and NbN layers, high purity Ti (99.95%) and Nb (99.99%) targets were sputtered for different durations in high purity Ar (99.999%) and N₂ (99.999%) plasma. The flow rates of nitrogen (η_{N_2}) and argon were controlled by mass flow controllers. Typically, TiN/NbN multilayers were deposited at a substrate temperature of 400°C and a pressure of $\sim 4.0 \times 10^{-3}$ mbar. A substrate bias of –200 V was applied to improve the mechanical properties of the coatings. The growth rates were 2 Å/sec each for TiN and NbN. These parameters were arrived at after doing a series of experiments involving variations of sputtering power, substrate bias, substrate temperature and operating pressure. The total thicknesses of the films were about 1.5 µm. Reproducible multilayer coatings with desired modulation wavelengths were obtained by a computer operated substrate rotation assembly, which controlled the dwell time of the substrate underneath each target very precisely.

The XRD data of the films were recorded in a Rigaku D/max 2200 X-ray powder diffractometer. The hardness measurements were performed using a nanoindenter (CSEM Instruments) at a load of 5 mN with a Berkovich diamond indenter. At this load the indentation depth was much less than 1/10th of the coating thickness, thus eliminating the effect of substrate on the hardness measurements. The corrosion behaviours of the coatings were studied in 0.5 M HCl solution by potentiodynamic polarisation technique. Thermal stability of the coatings was studied by vacuum annealing the coatings (T_a) at 100–850°C and recording the *in situ* XRD data in a high-temperature XRD machine.

3.0 Results and Discussion

3.1 XRD of Single Layer NbN and TiN Coatings

As NbN exists in different phases and additionally exhibits a limited range of nitrogen concentration wherein stoichiometric phases of TiN and NbN with B1 (NaCl) structure exist, the process parameters were first optimised for the deposition of single phase cubic TiN and NbN. This involved variations of nitrogen flow rate, sputtering power, operating pressure, substrate temperature and substrate bias. Figure 1 shows the XRD data of ~ 1 µm thick niobium nitride coating deposited at different nitrogen flow rates. The sputtering power was 110 W and the substrate bias was –200 V for all the coatings. For $\eta_{N_2} \geq 1.0$ sccm, hexagonal phase of niobium nitride was formed. For $\eta_{N_2} = 1.5$ sccm cubic phase of NbN was formed

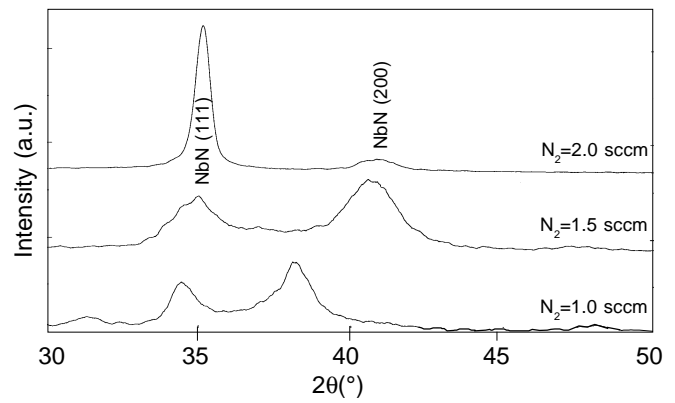


Fig. 1: XRD patterns of niobium nitride coatings deposited at various nitrogen flow rates.

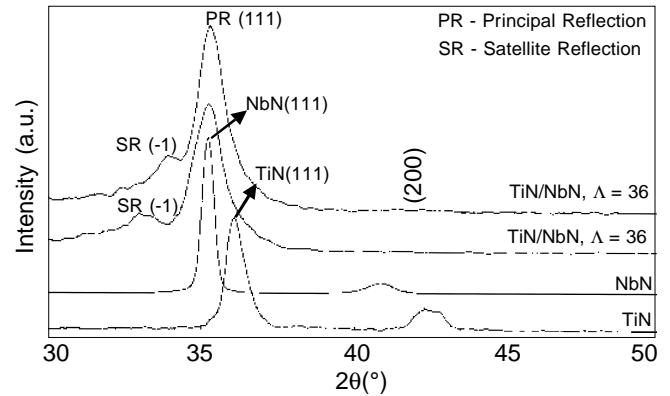


Fig. 2: XRD patterns of: (a) a single layer TiN coating (b) a single layer NbN coating and (c) TiN/NbN multilayer coatings with modulation wavelengths of 36 and 52 Å.

Author:

Amorphous?

Editor:

but the peaks were very broad and diffused, **indicating presence of defects** in the coating. At 2.0 sccm flow rate of nitrogen very high intensity (111) reflection of NbN was observed. For titanium nitride (results not shown), on the other hand, the films showed cubic phase with {111} texture in the entire N₂ concentration range (i.e., 2.0 sccm $\geq \eta_{N_2} \geq 1.0$ sccm). (Note that the sputtering power was 220 W and the substrate bias was –200 V for all TiN coatings). This showed that for $\eta_{N_2} = 2.0$ sccm both TiN and NbN coatings exhibited {111} texture. A nitrogen flow rate of 2.0 sccm was, thus, used for all the multilayer depositions.

3.2 XRD of TiN/NbN Multilayer Coatings

Figure 2 shows the XRD data of a typical single layer TiN coating, a single layer NbN coating and two TiN/NbN multilayer coatings deposited on Si (111) substrates. For the multilayer coatings the modulation wavelengths were 36 and 56 Å. All the coatings showed NaCl B1 structure with {111} texture. At lower bilayer thicknesses, the structure of the multilayers was composed of a (111) principal reflection,

which was flanked by 1st order negative satellite reflection, indicating the formation of superlattice structure under these conditions. For the multilayer coatings the full-width-at-half-maximum was higher as compared to the single layer TiN and NbN coatings, suggesting a smaller grain size. The average grain size of the multilayer coatings, as determined from the XRD data, was ~8–10 nm, whereas for TiN and NbN coatings it was ~15–16 nm.

Author:

Reference

3.3 Hardness of TiN/NbN Multilayer Coatings Editor.

Load vs. displacement curves were measured for single layer TiN and single layer NbN, and TiN/NbN multilayer samples. Typical plots obtained for three samples and the substrates are shown in Figure 3. After initial contact of the indenter on surface, the load was increased at a predetermined rate (10 mN/min) to the desired maximum load (5 mN) and then decreased at the same rate (10 mN/min) to zero. The unloading curve followed the partial elastic recovery of the sample material. From this plot the hardness was calculated using **Oliver and Pharr** method. The area formed by loading and unloading curves, defined as plastic deformation work (W_p), can be used to assess the resistance of plastic deformation and wear resistance of the coatings. The resistance of plastic deformation is inversely proportional to the plastic deformation work. In the present study, TiN/NbN multilayer coating showed the smallest plastic deformation and the largest resistance to plastic deformation as compared to the single layer TiN and NbN coatings. For the softest film (i.e., NbN), the maximum indentation depth was 120 nm, which was about 1/10th of the coating thickness. For the hardest film (i.e., TiN/NbN), the maximum indentation depth was only 70 nm.

The nanoindentation hardness variation of TiN/NbN multilayers as a function of modulation wavelength is shown in Figure 4. The measured hardnesses for NbN and TiN coatings deposited under the similar conditions were 1800 and 2400 kg/mm² respectively. The maximum measured hardness for TiN/NbN superlattice was 4000 kg/mm², which is ~2 times the rule-of-mixtures value. In the modulation wavelength range 400 Å > Λ > 20 Å, the hardness peaked at $\Lambda = 48$ Å. At very low and very high Λ , the hardness decreased. The decrease in hardness is probably due to the loss of superlattice structure under these conditions. This was supported by XRD data, which showed the loss of superlattice structure for films having 20 Å $\geq \Lambda \geq 150$ Å.

The enhancement in the hardness of TiN/NbN multilayer coating at low modulation wavelengths (150 Å $\geq \Lambda \geq 30$ Å) is attributed to the dislocations. As the thicknesses of the individual layers are very small, generation of dislocations (such as Frank Reed) cannot take place inside a given layer.⁸ Even if the dislocations are generated in a layer they cannot propagate along the growth direction because the interfaces act as the barrier for the propagation of dislocations. Furthermore, there is a large difference between the dislocation line energies for TiN and NbN because of large difference between the shear moduli of TiN (168 GPa) and NbN (104 GPa).⁵ This prevents the dislocation glide across the interfaces and hence pinning of dislocations at the interfacial sites. These two factors are believed to be

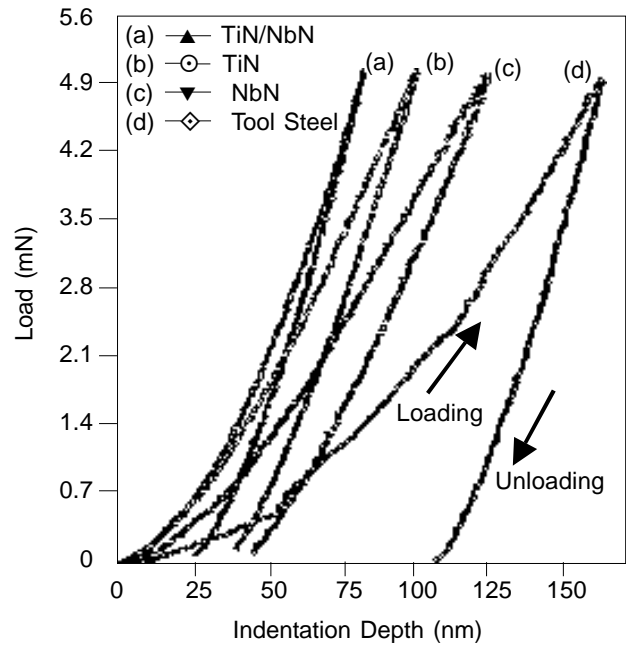


Fig. 3: Schematic representations of load vs. displacement curves at 5 mN load for (a) a TiN/NbN multilayer coating (b) a TiN coating (c) a NbN coating and (d) a tool steel substrate.

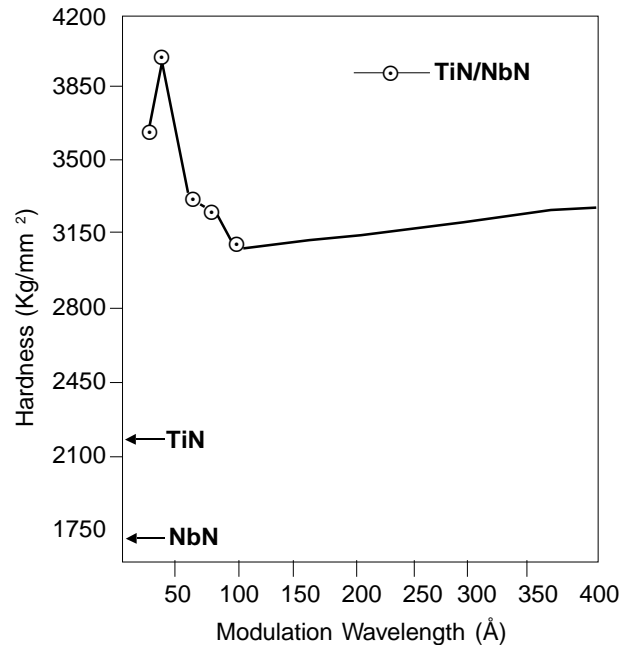


Fig. 4: Variation of nanoindentation hardness of TiN/NbN multilayer coatings with modulation wavelength. Also, shown are the hardnesses of single layer TiN and single layer NbN coatings.

responsible for the enhanced mechanical properties of the TiN/NbN multilayer coatings.

3.4 Thermal Stability of TiN/NbN Multilayers

TiN/NbN ($\Lambda = 50 \text{ \AA}$) multilayer coatings deposited on silicon substrate was annealed at 100–850°C for 30 minutes. Typical high-temperature XRD plots obtained from a TiN/NbN multilayer sample annealed at 400, 500, 600, 700, 800 and 850°C are shown in Figure 5. All the plots exhibited strong (111) principal reflection. First and 2nd order negative satellites and 1st order positive satellite were seen along the (111) principal peak. The XRD data were deconvoluted using a Peak Fit program to calculate the peak position, the peak intensity and the FWHM of the principal and the satellite reflections. The normalised intensity (I_{-1}/I_B) and FWHM of 1st order negative satellite reflection, for example, can be used to determine the quality of the superlattice coating after annealing.⁵ No significant change in I_{-1}/I_B was observed up to 700°C, however, it decreased significantly for $T_a > 700^\circ\text{C}$. Similarly, FWHM of the **SR** peak increased considerably for $T_a \geq 700^\circ\text{C}$. Both these observations indicated that the coating perfectly retained its superlattice character up to 700°C and subsequently started degrading marginally. The position of the satellite reflection did not change with annealing temperature, indicating no change in the modulation wavelength. Hence, variations in the layer thicknesses were minimal during annealing.

Author:

What is this?

3.5 Corrosion Behaviour of TiN/NbN Multilayers

Editor.

The corrosion behaviour of the coatings in 0.5 M HCl was studied using the potentiodynamic polarisation technique. The corrosion potential (E_{corr}) and corrosion current density (I_{corr}) obtained from these plots are presented in Figure 6. After coating the substrate with $\sim 1.5 \mu\text{m}$ thick TiN/NbN multilayer ($\Lambda = 50 \text{ \AA}$), E_{corr} increased from -0.460 to -0.340 V, whereas, I_{corr} decreased from 240 to $0.9 \mu\text{A}/\text{cm}^2$. Single layer TiN and NbN coatings exhibited almost similar corrosion behaviour with corrosion currents of 1.2 and $1.6 \mu\text{A}/\text{cm}^2$, respectively. The AFM images showed that before corrosion, the substrate exhibited very smooth surface morphology with a roughness of $\sim 4.6 \text{ nm}$. After corrosion, the substrate became very rough and R_a increased to $\sim 266 \text{ nm}$. Substrate coated with TiN/NbN multilayers exhibited a roughness of $\sim 5.2 \text{ nm}$ and it did not change even after corrosion in 0.5 M HCl solution ($\sim 5.4 \text{ nm}$ after corrosion), suggesting minimal chemical attack of the substrate and the coating.

In order to see the effect of interfaces on the corrosion behaviour of multilayers, the number of layers in the coatings were varied from 4 to 834, while maintaining a total coating thickness of $\sim 1.5 \mu\text{m}$. The corrosion current decreased from 1.3 to $0.6 \mu\text{A}/\text{cm}^2$ as the number of layers increased from 4 to 834. Similarly, the corrosion potential increased from -0.370 to -0.345 V. The variations of I_{corr} and E_{corr} with total number of layers are also plotted Figure 6. Though, these variations are not very large the trend of the two curves indicated that corrosion behaviour of the multilayers improved with more number of layers and reflects the reduced porosity of the

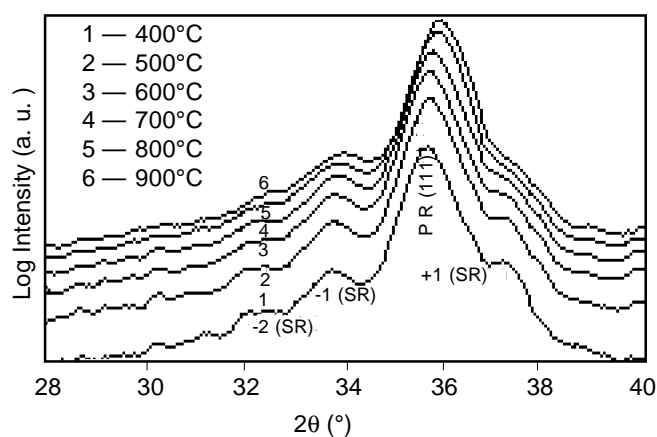


Fig. 5: High temperature XRD data of a TiN/NbN superlattice coating annealed at 400, 500, 600, 700, 800 and 850°C. The modulation wavelength was 50 \AA .

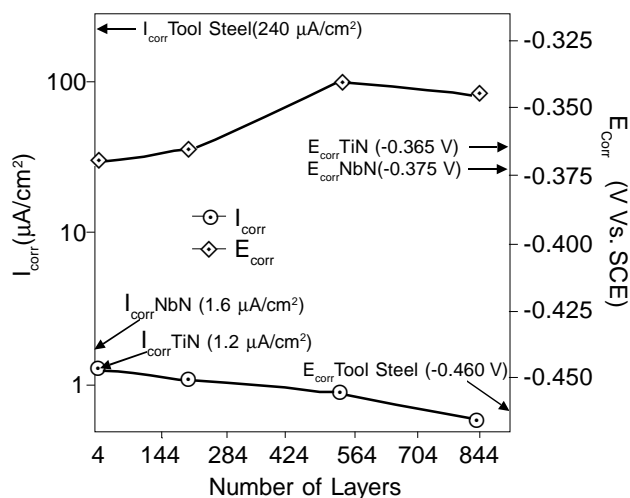


Fig. 6: Variations of I_{corr} and E_{corr} of TiN/NbN multilayers with total number of layers in 0.5 M HCl solution. Also shown are the values for tool steel substrate, single layer TiN and single layer NbN coatings.

coatings. As compared to bare substrate, about $1.5 \mu\text{m}$ thick TiN/NbN multilayer thus exhibited 400 times higher corrosion resistance. Similar improvement in the corrosion behaviour of multilayers has been reported in the literature.⁹ Lower values of corrosion currents even for the single layer coatings suggested that the microstructure of the coatings was highly dense and homogeneous. The SEM micrographs in planar view showed no evident corrosion attacks on the coatings. The dense microstructure of the coatings can be attributed to - ion bombardment during deposition, lower growth rates ($\sim 2 \text{ \AA}/\text{sec}$) and moderately higher deposition temperature (400°C). These parameters resulted in a fine-grained morphology of the coatings, as confirmed by AFM and XRD studies.

The present work demonstrates that layering of the two materials on nanometer scale not only improves the mechanical properties but also the thermal and chemical stability as compared to the single layer coatings. This approach has a great potential for designing new materials with tailored properties.

4.0 Conclusions

A reactive DC magnetron sputtering system was used to deposit nanostructured TiN/NbN multilayer coatings on silicon and tool steel substrates at various modulation wavelengths. Judicious control of the process parameters resulted in the deposition of polycrystalline TiN/NbN multilayer coatings with B1 NaCl fcc structure. The X-ray diffraction data showed that the coatings exhibited a superlattice structure for a modulation wavelength such that $40 \text{ \AA} \leq \Lambda \leq 106 \text{ \AA}$ with $\{111\}$ texture. Nanoindentation data showed that for the films prepared at $\Lambda = 48 \text{ \AA}$ and $V_B = -200 \text{ V}$ the hardness was as high as 4000 kg/mm^2 , which was about ~ 2 times the rule-of-mixtures value. High-temperature XRD data of the annealed TiN/NbN multilayer showed that the coating retained its superlattice structure up to 700°C and indicated a degradation in the quality of the coating for temperature higher than 700°C . The multilayer coatings exhibited a 400 fold decrease in I_{cor} compared to the uncoated steel substrate in 0.5 M HCl solution. The present work shows that TiN/NbN superlattices not only possess superior mechanical properties but also superior thermal and chemical properties.

5.0 Acknowledgements

The Department of Science and Technology and Council of Scientific and Industrial Research, New Delhi supported this research. Authors thank Dr. Anjana Jain for help in recording the XRD data. Mr. Aithu Poojari is thanked for corrosion measurements.

6.0 References

1. S.A. Barnett and A. Madan, *Physics World*, 1998, pp.45–50.
2. H.C. Barshilia, A. Jian and K.S. Rajam, *Vacuum*, in press.
3. H.C. Barshilia and K.S. Rajam, *Surface and Coatings Technology*, (accepted for publication).
4. H.C. Barshilia and K.S. Rajam, *Bulletin of Materials Science*, **26**(2), 2003, pp.233–237.
5. M. Shinn and S.A. Barnett, *Journal of Materials Research*, **7**(4), 1992, pp.901–911.
6. X. Chu, M.S. Wong, W.D. Sproul, S.L. Rohde and S.A. Barnett, *Journal of Vacuum Science and Technology A*, **10**(4), 1992, pp.1604–1609.
7. H.C. Barshilia and K.S. Rajam, *Surface and Coatings Technology*, **115**, 2002, pp.195–202.
8. J.S. Koehler, *Physical Review B*, **2**(2), 1970, pp.547–551.
9. M. Nordin, M. Herranen and S. Hogmark, *Thin Solid Films*, **348**, 1999, pp.202–207.